which suppresses the negative contributions for the large velocities in question.

To fix our arguments, we introduce a velocity bound $C_{\max}$ defined such that $f \simeq 0$ for $C > C_{\max}$ and demand that

$$\Phi > -1 \qquad \text{for} \qquad C < C_{\max} \tag{6}$$

Because of the polynomial structure of Φ, this requirement is tantamount to

$$|\Phi| < 1 \qquad \text{for} \qquad C < C_{\max} \tag{7}$$

With this in mind, we turn the attention to the entropy production Eq. (2). Because of conservation of mass, momentum, and energy, $\int \mathcal{S} \ln f_M \, \mathrm{d}\boldsymbol{c} = 0$ (Ref. 7), and we find the entropy production as

$$\sigma = -k \int \mathcal{S} \ln(1 + \Phi) \, \mathrm{d}\boldsymbol{c} \tag{8}$$

This equation makes sense under the assumption that $C_{\max}$ is a suitable bound for the collision term $\mathcal{S}$ as well so that $\mathcal{S}$ is negligible above $C_{\max}$, where the argument of the logarithm becomes negative.

The condition of Eq. (7) is the prerequisite for expanding the logarithm into a Taylor series, namely,

$$\sigma = -k \int \mathcal{S} \left(\Phi - \frac{\Phi^2}{2} + \cdots \right) \mathrm{d}\boldsymbol{c}$$

$$= -k \int \mathcal{S} \left\{ Kn\phi^{(1)} + Kn^2 \left[-\frac{1}{2} \left(\phi^{(1)} \right)^2 + \phi^{(2)} \right] + \cdots \right\} \mathrm{d}\boldsymbol{c} \tag{9}$$

We emphasize that the series does not converge if $|\Phi| \geq 1$. In other words, the series expansion is wrong if the requirement of Eq. (7) is violated.

Thus, if Eq. (7) holds, everything turns out well. In particular, we are allowed to compute the entropy production by means of the expansion in Eq. (9). On the other hand, if Eq. (7) is not fulfilled, the expansion is not allowed and will, if used, give incorrect results, for example, a negative value for the entropy production. This, indeed, is the explanation for the results of Ref. 1, where the preceding expansion is used, but the finite radius of convergence is left out of consideration.

Clearly, the condition of Eq. (7) is not easy to evaluate, in particular because one has to provide the bound $C_{\max}$ first. As an example, we consider the first Chapman–Enskog expansion for Maxwell molecules of Eq. (5). In this case the condition of Eq. (7) can be written as

$$\frac{\eta}{p} \left| \xi_i \xi_j \frac{\partial v_{\langle i}}{\partial x_{j \rangle}} \right| \leq 1, \qquad \frac{15}{4} \frac{\eta}{p\sqrt{(m/k)T}} \left| \xi_k \left(1 - \frac{\xi^2}{5} \right) \frac{\partial T}{\partial x_k} \right| \leq 1 \tag{10}$$

where ξ_i is a suitable dimensionless velocity with absolute value of the order of $C_{\max}/\sqrt{[(k/m)T]}$. The first of these conditions resembles the conditions of Ref. 1 for positive entropy production in the Burnett case, and we can consider our preceding arguments as the explanation of these conditions.

For the first-order expansion, however, only the first term in the series (9) is required for the entropy production

$$\sigma = -k \int \mathcal{S} \Phi \, \mathrm{d}\boldsymbol{c} \tag{11}$$

which turns out to be positive for all gradients of temperature and velocity.[3] Because the expansion is not allowed if the conditions of Eqs. (7) or (10) are violated, this result must be seen as a mere coincidence. See also Ref. 8, where the authors show that the realizability of some moments of the first-order Chapman–Enskog phase density is not ensured if the gradients become to steep.

Finally, we would like to point out that the computation of the entropy production from Grad's moment method faces similar problems.

Conclusions

We summarize our results as follows:

1) The Chapman–Enskog method does not ensure the positivity of the phase density in general. This poses no problem if the method is applied in the permitted range of processes.

2) A negative entropy production may occur as a result of a negative phase density and improper mathematics (nonconverging series).

3) Therefore, a negative entropy production shows that the approximation is overstressed and as such serves as an indicator for the applicability of the model.[1]

References

[1] Comeaux, K. A., Chapman, D. R., and MacCormack, R. W., "An Analysis of the Burnett Equations Based on the Second Law of Thermodynamics," AIAA Paper 95-0415, 1995.

[2] Cercignani, C., *Theory and Application of the Boltzmann Equation,* Scottish Academic Press, Edinburgh, 1975, pp. 40, 232.

[3] Chapman, S., and Cowling, T. G., *The Mathematical Theory of Non-Uniform Gases,* Cambridge Univ. Press, Cambridge, England, U.K., 1970, pp. 46, 107.

[4] Grad, H., "On the Kinetic Theory of Rarefied Gases," *Communications on Pure and Applied Mathematics*, Vol. 2, Wiley, New York, 1949, p. 231.

[5] Müller, I., and Ruggeri, T., *Rational Extended Thermodynamics* (*Springer Tracts in Natural Philosophy*, Vol. 37), 2nd ed., Springer-Verlag, New York, 1998, p. 19.

[6] Bobylev, A. V., "The Chapman–Enskog and Grad Methods for Solving the Boltzmann Equation," *Soviet Physics Doklady*, Vol. 27, No. 1, 1998, pp. 29–31.

[7] Liboff, R. L., *The Theory of Kinetic Equations*, Wiley, New York, 1969, p. 263.

[8] Levermore, C. D., Morokoff, W. J., and Nadiga, B. T., "Moment Realizability and the Validity of the Navier–Stokes Equations for Rarefied Gas Dynamics," *Physics of Fluids*, Vol. 10, No. 12, 1998, pp. 3214–3226.

Resolution of Magnetogasdynamic Phenomena Using a Flux-Vector Splitting Method

Patrick W. Canupp*
Air Force Research Laboratory,
Wright–Patterson Air Force Base, Ohio 45433-7542

Nomenclature

A_p	=	Powell's flux-vector Jacobian
$\hat{a}$	=	homogeneity variable
$\boldsymbol{B}$	=	magnetic field vector
$\boldsymbol{b}$	=	unsplit flux
C	=	left eigenvector matrix
C^{-1}	=	right eigenvector matrix
c_v	=	constant-volume specific heat
$\boldsymbol{F}$	=	x-direction flux vector
p	=	pressure
R	=	gas constant
R_n	=	nose radius
S	=	transformation Jacobian from conservative to primitive variables
$\boldsymbol{S}$	=	cell-face surface area
S^{-1}	=	transformation Jacobian from primitive to conservative variables
T	=	temperature
$\boldsymbol{U}$	=	conservative variables vector

Received 7 August 2000; revision received 5 February 2001; accepted for publication 6 February 2001.

* Visiting Research Scientist, Computational Sciences Branch; also Senior Research Associate, Ohio Aerospace Institute. Member AIAA.

$\boldsymbol{u}$ = velocity vector
u, v, w = velocity components
V = velocity magnitude
$\boldsymbol{V}$ = primitive variables vector
$\mathcal{V}_i$ = volume of the ith cell
Z = mass-specific total energy
γ = ratio of specific heats
Λ = diagonal eigenvalue matrix
$\Lambda_\pm$ = positive and negative eigenvalue matrices
ρ = mass density

Subscripts

x, y, z = components in the x, y, or z directions
∞ = freestream condition

Introduction

INTEREST in hypersonic flight has renewed research in plasma aerodynamics and magnetogasdynamics (MGD). The goals of such research include controlling the plasma in a weakly ionized flow field to reduce vehicle drag and thermal loading. In 1959, Ziemer experimentally demonstrated that an applied magnetic field increased shock stand-off distance for hypersonic plasma flow over a blunt body.[1] Although this and other experiments have demonstrated plasma effects in compressible flows, the mechanisms responsible for the observed changes remain a subject of debate; therefore, numerical simulation provides valuable input for plasma aerodynamics research.

The MGD equations combine the equations of fluid flow with Maxwell's equations of electromagnetics. Several investigators have developed numerical methods for solving the ideal MGD equations, which are essentially an inviscid set of equations with infinite electrical conductivity.[2–6] In their seminal work Brio and Wu devised a one-dimensional approximate Riemann solver for the ideal MGD equations.[2] Powell later extended their work to two dimensions with a method that avoided the singularity in the flux-vector Jacobians by introducing source terms that are proportional to magnetic field divergence.[3,4]

More recently, MacCormack cleverly redefined the ideal MGD flux vectors to make them homogeneous of degree one to devise a flux-vector splitting method.[7] Conveniently, the newly defined fluxes result in a set of Jacobians that reduce to those studied earlier by Powell. MacCormack used the eigensystem of Powell[3] in his conservation-form method to compute a three-dimensional, viscous, blunt-body flow. The results of his study were inconclusive because of uncertainties in proper magnetic field boundary conditions.

The present research modifies MacCormack's MGD flux-vector splitting method by adopting the robust eigensystem of Powell et al.[4] Because of uncertainties in the results presented for the complex flow in Ref. 7, the current effort seeks solutions to simpler problems. In particular, this work validates the new method by computing the MGD shock tube problem and also examines the effects of magnetic field on a two-dimensional MGD blunt-body flow.

Numerical Method

The MGD equations are the traditional Navier–Stokes equations of fluid dynamics modified to account for magnetic force effects and Joule heating. Assuming infinite electrical conductivity and neglecting viscous stress and heat transfer, the one-dimensional ideal MGD equations take the following vector form:

$$\frac{\partial \boldsymbol{U}}{\partial t} + \frac{\partial \boldsymbol{F}}{\partial x} = 0 \tag{1}$$

MacCormack[7] redefines the vector of conserved quantities as

$$\boldsymbol{U} = (\rho, \rho u, \rho v, \rho w, \rho Z, B_x, B_y, B_z, \hat{a})^T \tag{2}$$

and the inviscid flux vector as

$$\boldsymbol{F} = \begin{bmatrix} \rho u \\ \rho u^2 + p + B^2/2\hat{a} - B_x(B_x/\hat{a}) \\ \rho uv - B_y(B_x/\hat{a}) \\ \rho uw - B_z(B_x/\hat{a}) \\ (\rho Z + p + B^2/2\hat{a})u - (\boldsymbol{B}\cdot\boldsymbol{u})(B_x/\hat{a}) \\ B_x u - uB_x \\ B_y u - vB_x \\ B_z u - wB_x \\ 0 \end{bmatrix} \tag{3}$$

The quantity $\hat{a}$ conveniently makes $\boldsymbol{F}$ homogeneous of degree one in $\boldsymbol{U}$ and remains constant throughout the domain. The total energy density in the gas is

$$\rho Z = \rho c_v T + B^2/2\hat{a} + \tfrac{1}{2}\rho V^2 \tag{4}$$

and the pressure is

$$p = \rho R T \tag{5}$$

The discretized version of Eq. (1) for a set of finite volumes is

$$\frac{\delta \boldsymbol{U}_i}{\Delta t}\mathcal{V}_i + \sum_{\text{sides}} S^{-1}\left(S\frac{\partial \boldsymbol{F}}{\partial \boldsymbol{V}}\right)S\boldsymbol{U}\cdot\boldsymbol{S} = 0 \tag{6}$$

where the summation takes place over the cell interfaces. The flux consists of two components

$$\boldsymbol{F} = \begin{bmatrix} S^{-1}A_p S\boldsymbol{U} \\ 0 \end{bmatrix} + \begin{bmatrix} \boldsymbol{b} \\ 0 \end{bmatrix}\hat{a} \tag{7}$$

where $\boldsymbol{U}$ is the eight-element vector of conserved variables (without $\hat{a}$) and A_p denotes Powell's 8×8 matrix. Therefore, construction of the flux vector in Eq. (7) begins with splitting the component that involves the Powell matrix using its eigenvalues and eigenvectors. Choosing $\hat{a}$ to be unity gives the remaining flux:

$$\boldsymbol{b} = \big[0, (\gamma-2)(B^2/2), 0, 0, (\gamma-2)(B^2u/2), -uB_x, -vB_x, -wB_x\big]^T \tag{8}$$

which is formed by central averages.

Using a similarity transformation, Eq. (6) becomes

$$\frac{\delta \boldsymbol{U}_i}{\Delta t}\mathcal{V}_i + \sum_{\text{sides}} S^{-1}C^{-1}\Lambda C S\boldsymbol{U}\cdot\boldsymbol{S} + \sum_{\text{sides}} \boldsymbol{b}\cdot\boldsymbol{S} = 0 \tag{9}$$

The form of Eq. (9) allows easy identification of the split fluxes

$$\boldsymbol{F}_\pm = S^{-1}C^{-1}\Lambda_\pm C S\boldsymbol{U} \tag{10}$$

The columns of C^{-1} are identical to the right eigenvectors given in Powell et al.[4] The rows of C are the left eigenvectors, scaled to ensure that $CC^{-1} = I$. The present effort combines this eigensystem with MacCormack's flux-vector splitting approach to obtain a robust, one-dimensional MGD flow solver. The numerical method allows either first- or second-order spatial accuracy, and it is first-order accurate in time.

Computation of the MGD Shock Tube

The MGD shock-tube problem, originally proposed by Brio and Wu,[2] serves to validate the new flux-vector splitting method and illustrates its shock-capturing properties. In this problem gases at two different thermodynamic states interact through an unsteady system of five different waves. The conditions simulated in the current work match those of Brio and Wu,[2] and the results of the flux-vector splitting method are compared to those of the fourth-order compact-difference method of Gaitonde.[6]

Figure 1 shows the density distribution in the tube after 400 time steps. Labels mark the five different waves, which propagate into the undisturbed gas on either end of the shock tube, setting up two regions of flow (one to the right and one to the left), which meet at the slow shock. The compact scheme performs better than the flux-split

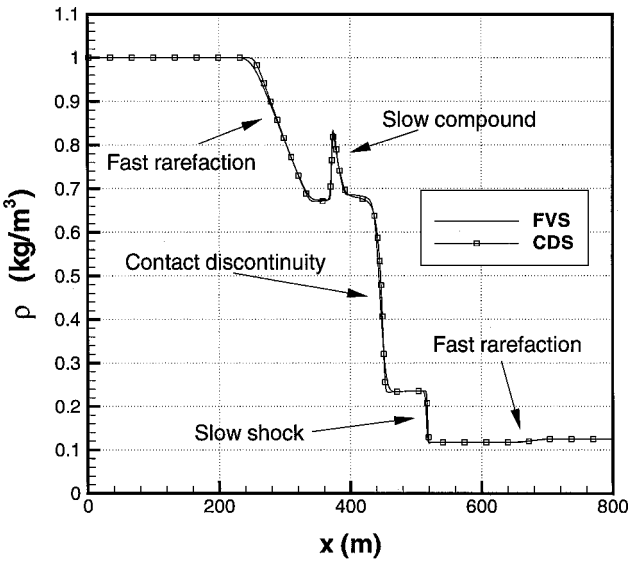

Fig. 1 Variation of density through the shock tube. FVS indicates results from the flux-vector splitting method, whereas CDS denotes results from the compact-difference method of Ref. 6.

method through the left-moving fast rarefaction and on the right side of the contact discontinuity. The flux-vector splitting method captures the flow between the contact discontinuity and the slow compound wave better than the compact scheme. However, the flux-vector splitting method is slightly more dissipative through the shock. The two methods predict nearly identical wave speeds for all of the waves in the flow. These results show that the new flux-vector splitting method accurately captures time evolution of the MGD equations. Even though the flux-split results come from a first-order version of the method, the small grid spacing on the 800-point grid provides enough resolution such that they almost identically match the fourth-order results of the compact-difference method.

Magnetic Field Effects on Blunt-Body Flow

An extension of the one-dimensional flux-split method using rotated flux vectors enables computation of two-dimensional flow over a cylindrical-nosed blunt body. The numerical method uses freestream boundary values, standard centerline symmetry conditions, inviscid boundary conditions at the body surface, and supersonic extrapolation conditions in the outflow plane. In addition, the method extrapolates magnetic field values at all but the freestream boundaries. At the freestream boundary the magnetic field values are constant. These calculations use second-order flux evaluation in the streamwise direction and first-order evaluation in the body-normal direction. Integration in time to steady-state continues until the solution residual reduces by nine orders of magnitude.

Figure 2 compares pressure contours for two Mach 5.85 hypersonic blunt-body flows with freestream conditions $p_\infty = 510$ Pa and $T_\infty = 55$ K. The flow in the upper portion of the figure has no applied magnetic field, whereas the lower portion of the figure presents results for which the freestream magnetic field directs out of the plane of flow along the positive z axis. For the case without the magnetic field, the bow shock wave stands at $0.45R_n$ away from the stagnation point on the stagnation streamline, which agrees well with the empirical result of $0.44R_n$ (Ref. 8). An imposed magnetic field at the freestream boundary $\boldsymbol{B} = 0.034\,\hat{k}T$ causes an approximately 42% increase in shock wave stand-off distance and reduces the thermodynamic pressure distribution on the body surface. However, the total pressure at the surface, which includes magnetic pressure, remains the same as in the case without magnetic field. These results indicate that the applied magnetic field will not change the overall wave drag. The calculation results shown in Fig. 2 are for a 200×200 grid. To demonstrate grid convergence, Fig. 3 shows results for the case with magnetic field on two different grids. The shock-wave shape is identical on the two grids, and the post-

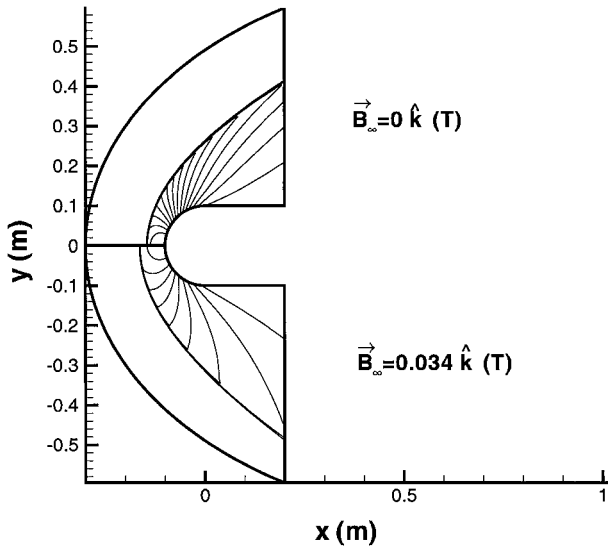

Fig. 2 Pressure contours for blunt-body flows with and without z-direction freestream magnetic field.

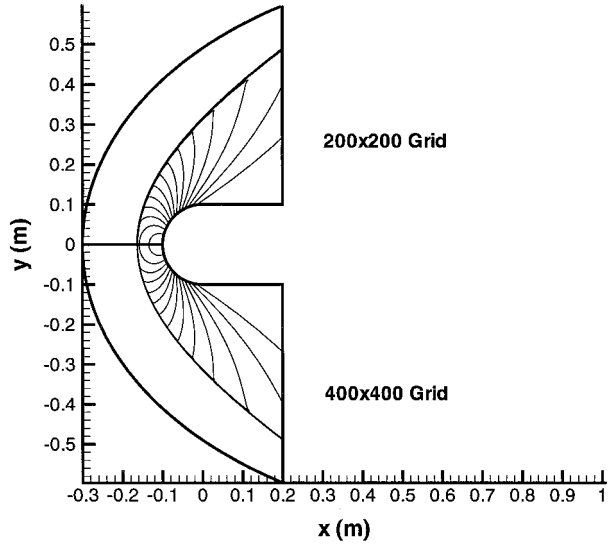

Fig. 3 Pressure contours for two different grids.

shock flow structure does not significantly change for higher grid resolution.

Conclusions

This research validates a one-dimensional flux-vector splitting algorithm for solving the unsteady ideal MGD equations. The results demonstrate that the method accurately simulates the unsteady phenomena associated with the MGD Riemann problem. A two-dimensional extension of the numerical method computes effects of magnetic field on hypersonic blunt-body flow. The applied magnetic field causes the bow shock wave to displace away from the body surface, but it does not change the total pressure distribution on the surface.

Acknowledgments

The author is grateful for Air Force Office of Scientific Research sponsorship under tasks monitored by W. Hilbun and S. Walker. The author thanks D. Gaitonde for providing data from his MGD shock-tube calculations for comparison purposes.

References

[1] Ziemer, R. W., "Experimental Investigation in Magneto-Aerodynamics," *American Rocket Society Journal*, Vol. 29, No. 9, 1959, pp. 642–647.

[2]Brio, M., and Wu, C. C., "An Upwind Differencing Scheme for the Equations of Ideal Magnetohydrodynamics," *Journal of Computational Physics*, Vol. 75, No. 2, 1988, pp. 400–422.
[3]Powell, K. G., "An Approximate Riemann Solver for Magnetohydrodynamics," NASA CR 194902, April 1994.
[4]Powell, K. G., Roe, P. L., Myong, R. S., Gombosi, T., and Zeeuw, D. D., "An Upwind Scheme for Magnetohydrodynamics," AIAA Paper 95-1704, June 1995.
[5]Augustinus, J., Hoffmann, K. A., and Shigeki, H., "Effect of Magnetic Field on the Structure of High-Speed Flows," *Journal of Spacecraft and Rockets*, Vol. 35, No. 5, 1998, pp. 639–646.
[6]Gaitonde, D. V., "Development of a Solver for 3-D Non-Ideal Magnetogasdynamics," AIAA Paper 99-3610, June 1999.
[7]MacCormack, R. W., "An Upwind Conservation Form Method for the Ideal Magnetohydrodynamics Equations," AIAA Paper 99-3609, June 1999.
[8]Billing, F. S., "Shock-Wave Shapes Around Spherical and Cylindrical-Nosed Bodies," *Journal of Spacecraft and Rockets*, Vol. 4, No. 6, 1967, pp. 822, 823.

Errata

Heat Transfer Predictions Using a Dual-Dissipation k–ε Turbulence Closure

U. Goldberg and P. Batten
Metacomp Technologies, Inc., Westlake Village, California 91361

[J. Thermophysics and Heat Transfer, 15(2), pp. 197–204 (2001)]

THE sentence that begins in the fourth-to-last line in the left-hand column on p. 200 was edited incorrectly, and should read as follows: "The cubic model overpredicts the wall heat transfer, whereas the three-equation closure predicts the peak level correctly."
AIAA regrets the error.